Electronic Supplementary Material (ESI) for Nanoscale.

Supporting Information

Title: 3D Self-supported $Ni(PO_3)_2$-MoO_3 Nanorods Anchored on Nickel Foam for Highly Efficient Overall Water Splitting

*Kai Li, Jingwen Ma, Xinglong Guan, Hongwei He, Min Wang, Guoliang Zhang, Fengbao Zhang, Xiaobin Fan, Wenchao Peng, Yang Li**

Experimental Section

Synthesis of Ni-P/NF

In order to demonstrate the role of the phosphorization step, the Ni-P/NF catalyst was also synthesized with the same method as for $Ni(PO_3)_2$-MoO_3/NF except for the addition of $(NH_4)_2Mo_2O_7 \cdot 4H_2O$ in preparation process.

Synthesis of Mo-P/NF

In order to demonstrate the role of the phosphorization step, the Ni-P/NF catalyst was also synthesized with the same method as for $Ni(PO_3)_2$-MoO_3/NF except for the addition of $Ni(NO_3)_2 \cdot 6H_2O$ in preparation process.

Electrochemical measurements

All the electrochemical measurements were tested with a CHI 660E electrochemistry workstation (CH Instruments, Inc., Shanghai) in a standard three-electrode system using a 1.0 M KOH (pH=13.6) aqueous solution. The Ag/AgCl in saturated KCl solution and graphite rod were used as reference and counter electrode, respectively. one piece of $Ni(PO_3)_2$-MoO_3/NF foam plate was directly use as working electrode. Polarization curves were obtained using linear sweep voltammetry (LSV) curves conducted with a scan rate of 5 mV s^{-1}. Electrochemical impedance spectroscopy (EIS) was tested with frequency from 10^6 to 0.01 Hz and an AC voltage of 10mV at -0.1 V *vs.* RHE.

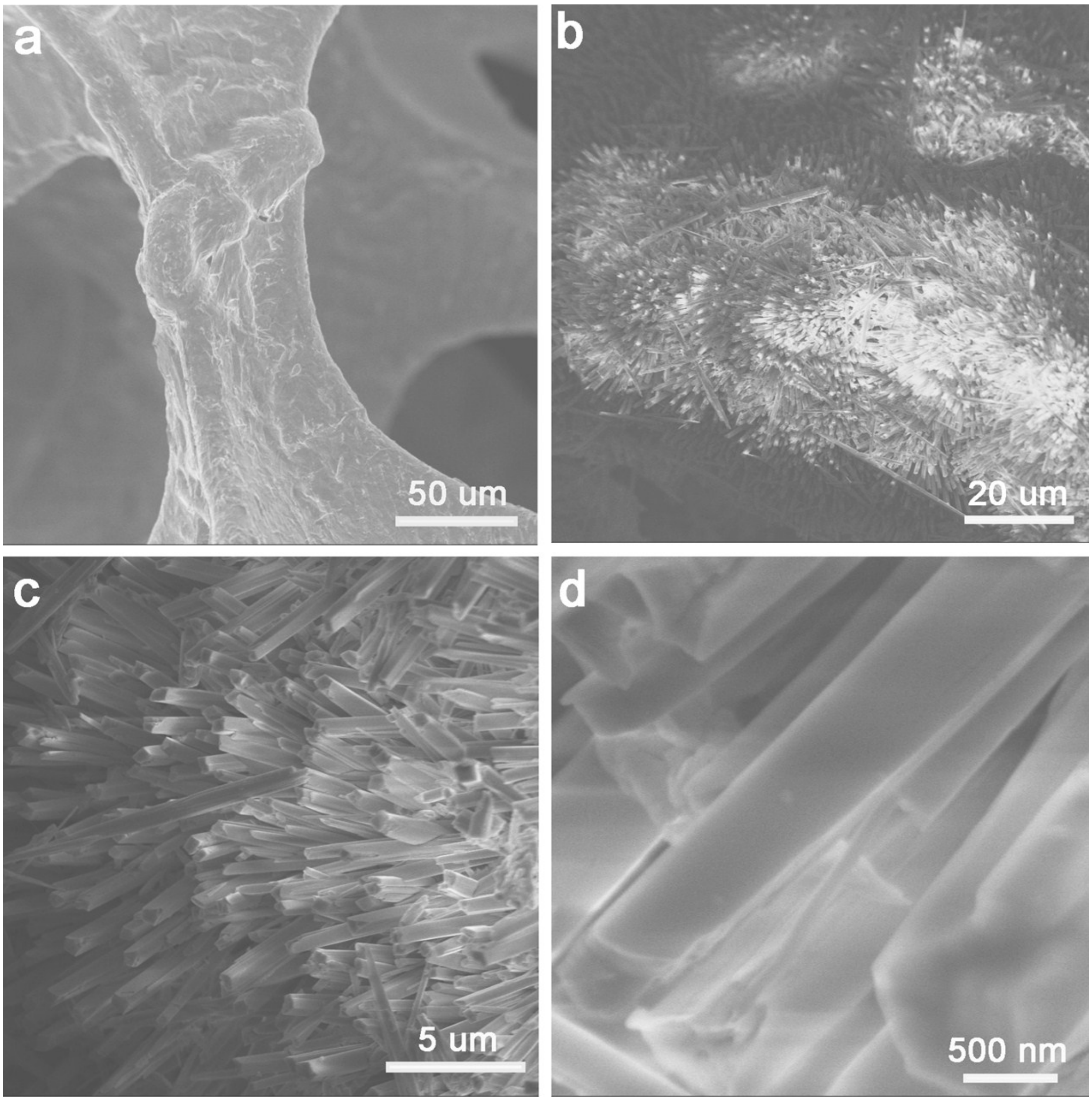

Figure S1. SEM images of (a) bare nickel foam and (b-d) $NiMoO_4$/NF.

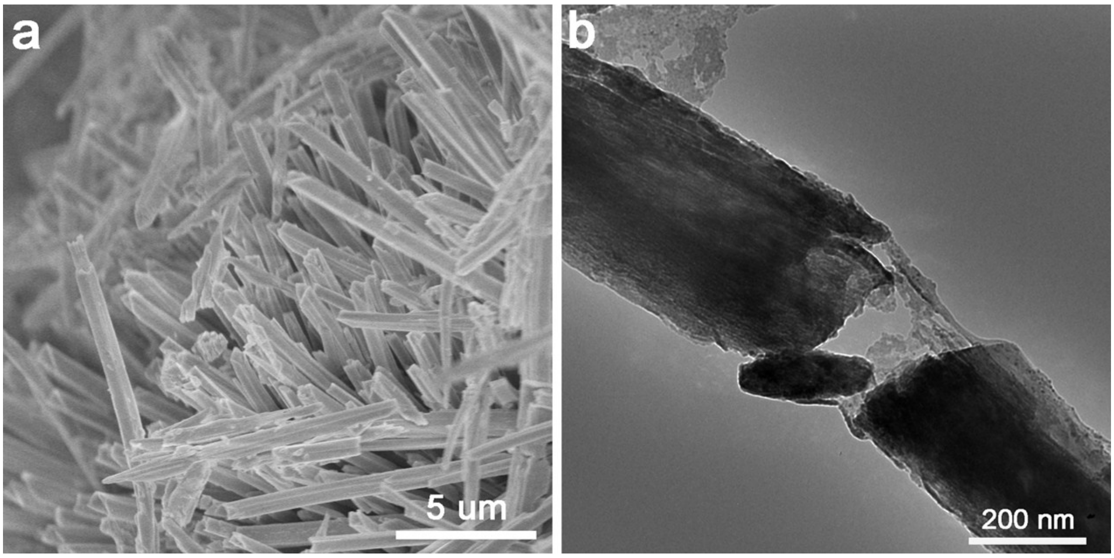

Figure S2. SEM image (a) and TEM images (b) of $Ni(PO_3)_2$-MoO_3/NF.

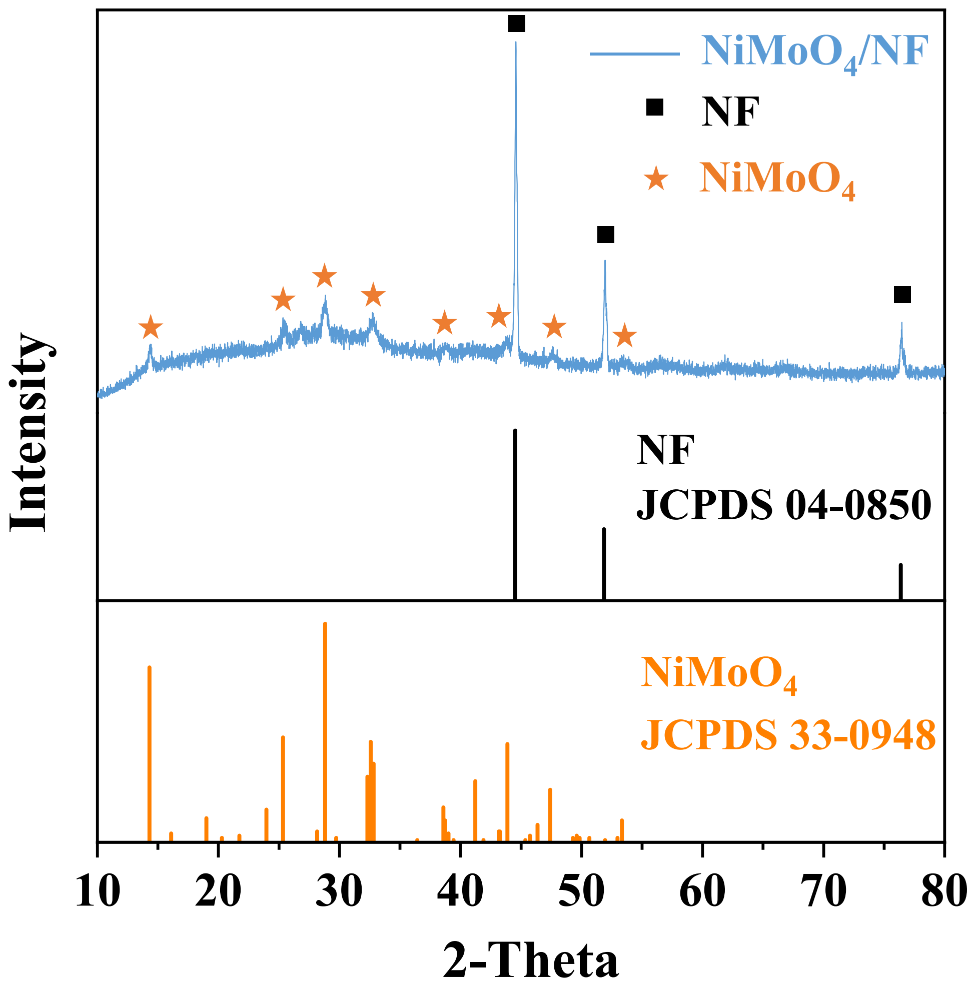

Figure S3. XRD patterns of $NiMoO_4$/NF.

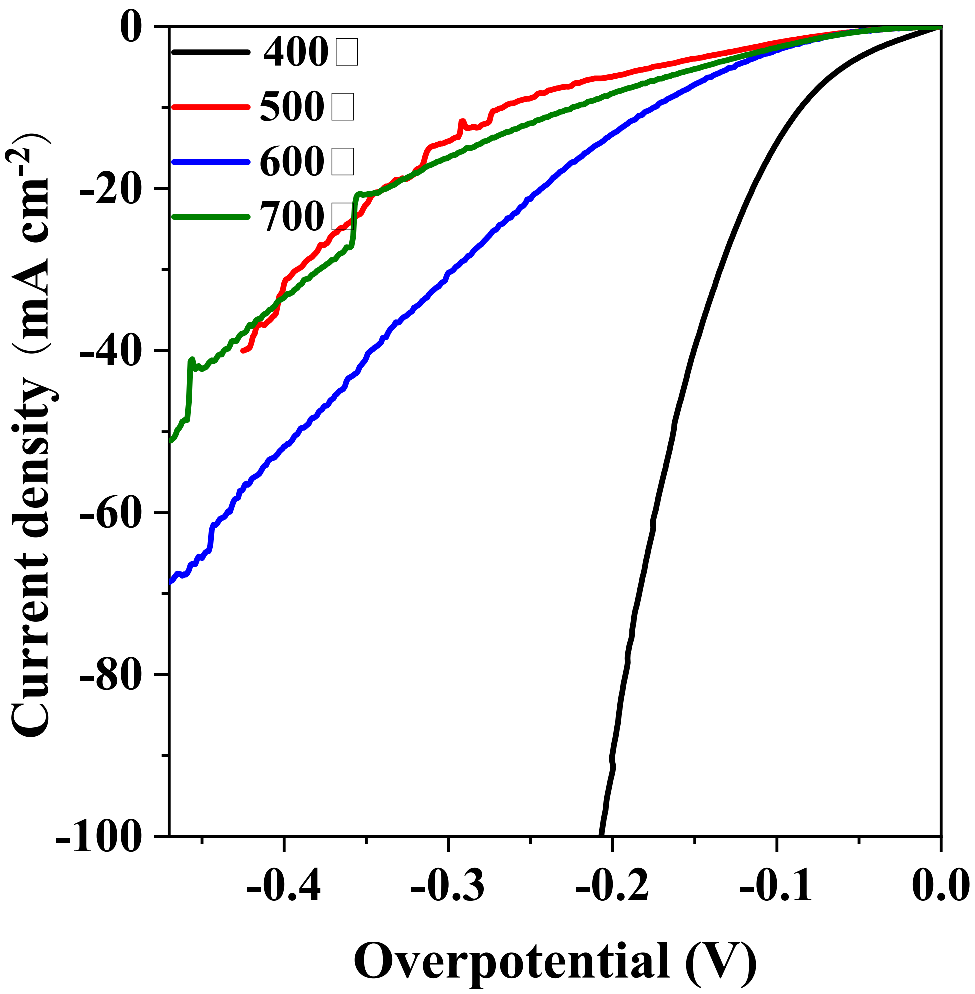

Figure S4. Polarization curves for HER of $Ni(PO_3)_2$-MoO_3/NF from different phosphating temperature.

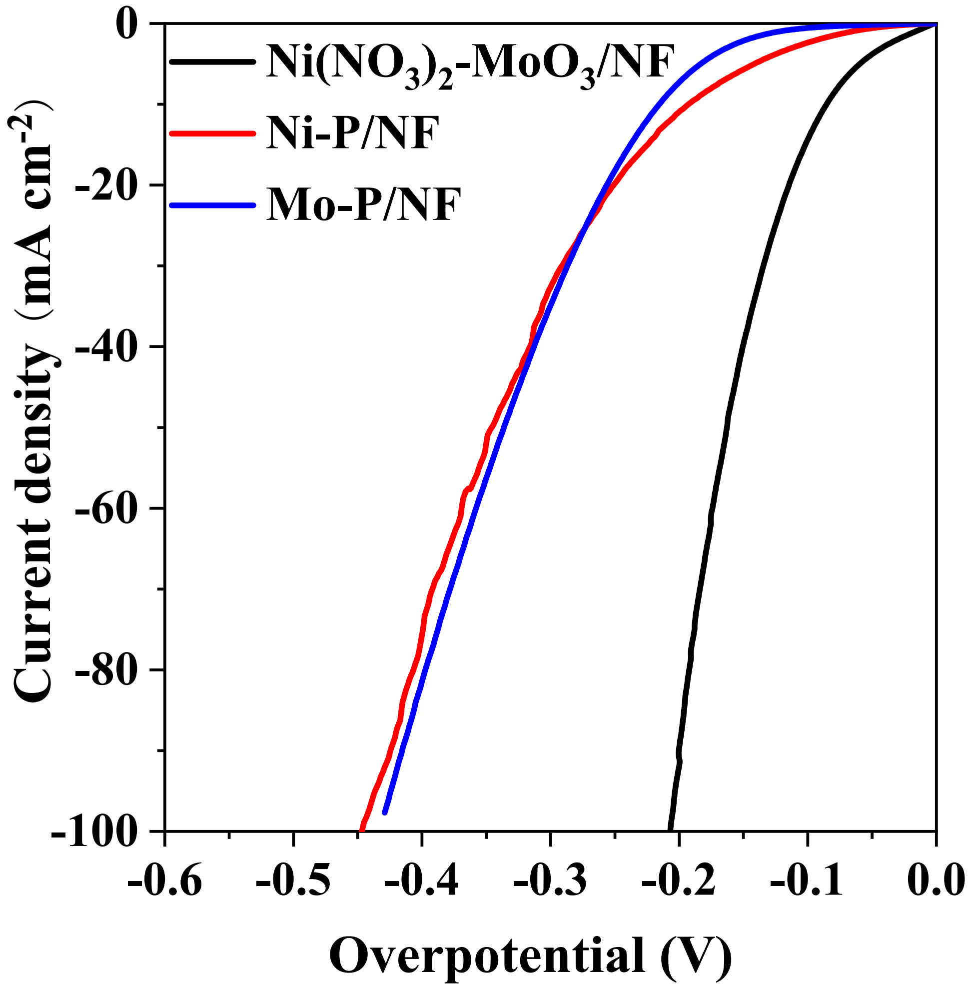

Figure S5. Polarization curves for HER of $Ni(PO_3)_2$-MoO_3/NF, Ni-P/NF and Mo-P/NF.

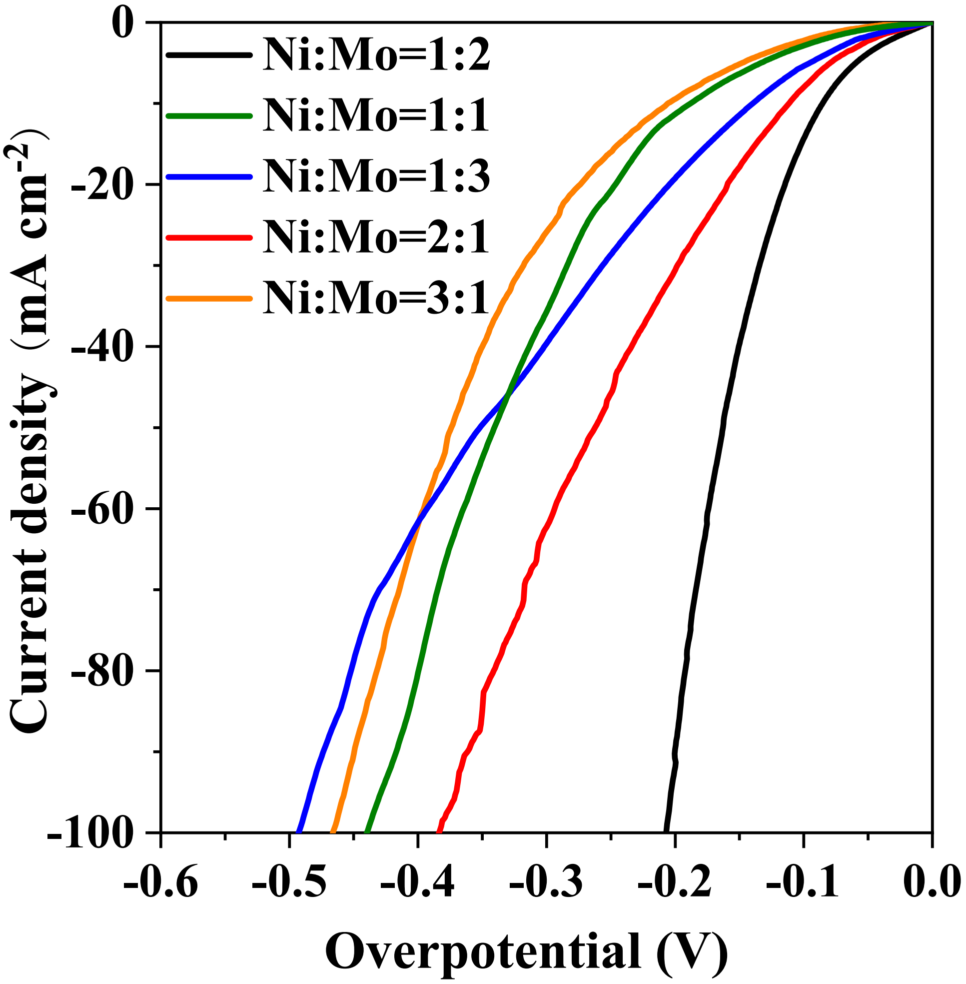

Figure S6. Polarization curves for HER of $Ni(PO_3)_2$-MoO_3/NF from different proportion of Mo and Ni by adjusting synthesis quantity of metal precursor.

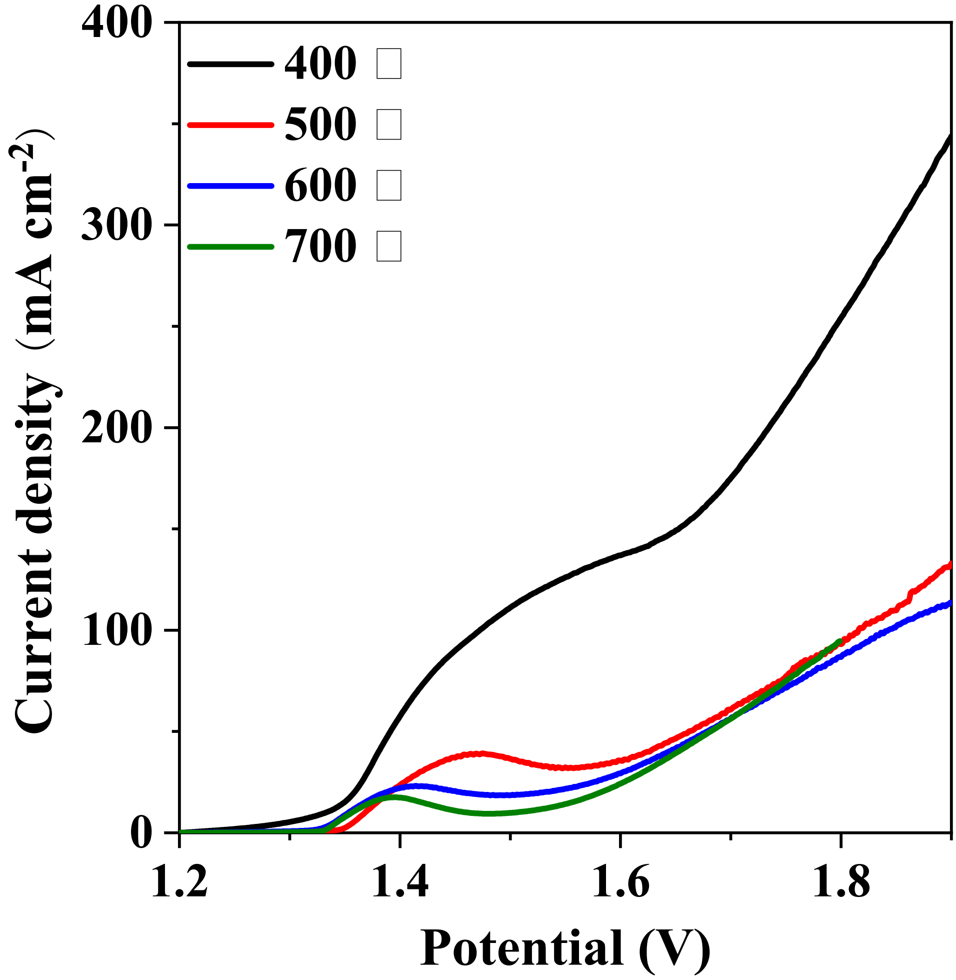

Figure S7. Polarization curves for OER of $Ni(PO_3)_2$-MoO_3/NF from different phosphating temperature.

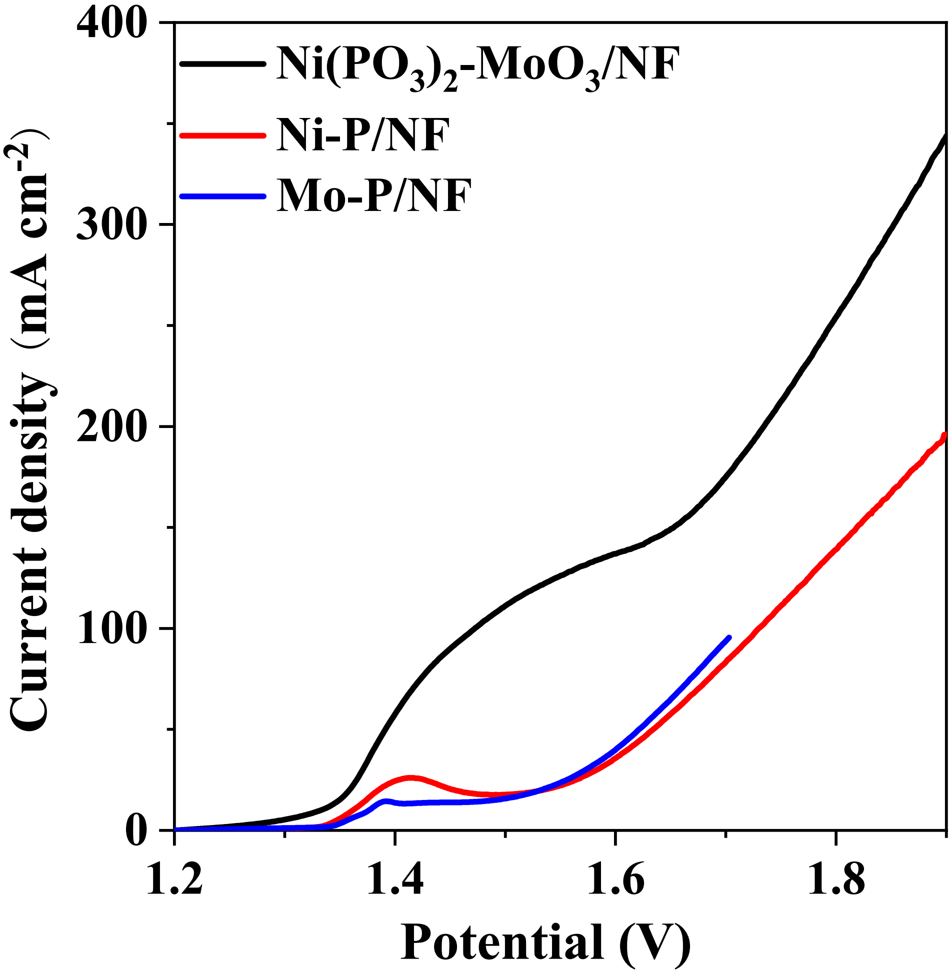

Figure S8. Polarization curves for OER of $Ni(PO_3)_2$-MoO_3/NF, Ni-P/NF and Mo-P/NF.

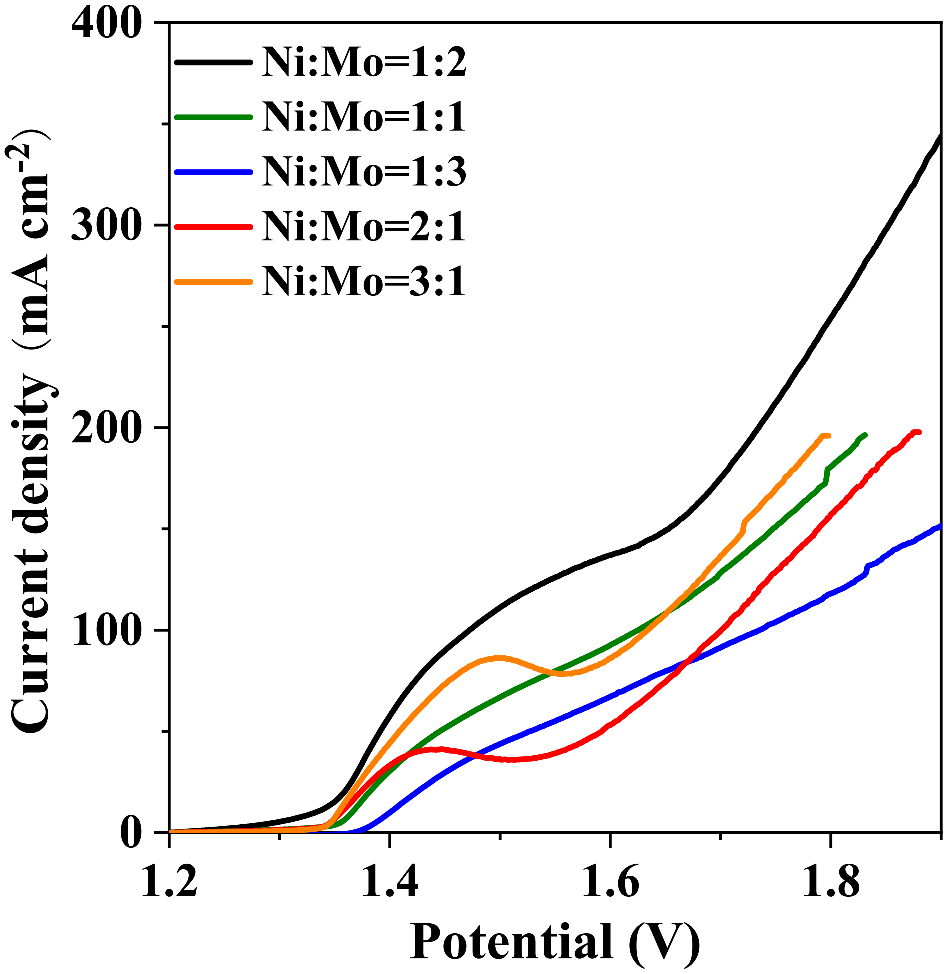

Figure S9. Polarization curves for OER of $Ni(PO_3)_2$-MoO_3/NF from different proportion of Mo and Ni by adjusting synthesis quantity of metal precursor.

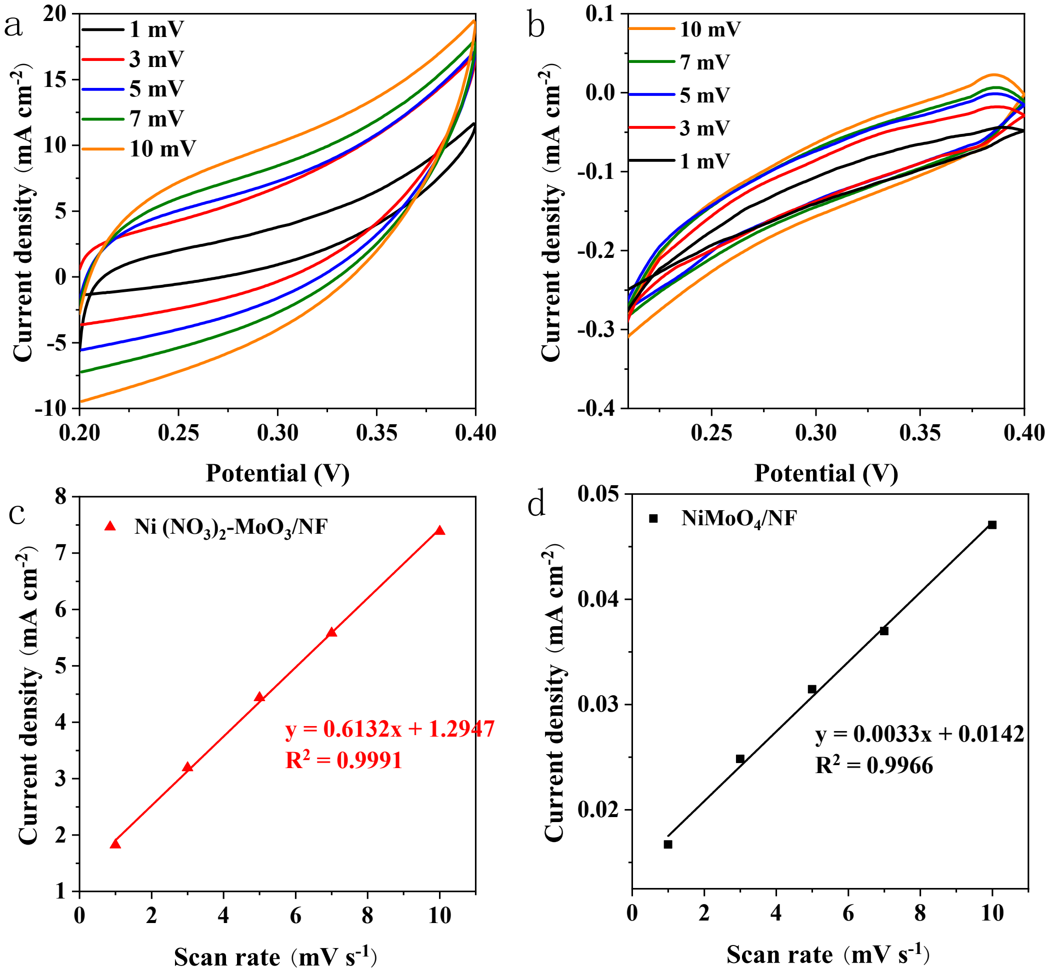

Figure S10. CV curves at different scan rates of (a) $Ni(PO_3)_2$-MoO_3/NF and (b) $NiMoO_4$/NF. The capacitive currents of (c) $Ni(PO_3)_2$-MoO_3/NF and (d) $NiMoO_4$/NF are measured at 0.30 V vs. RHE plotted as a function of scan rate.

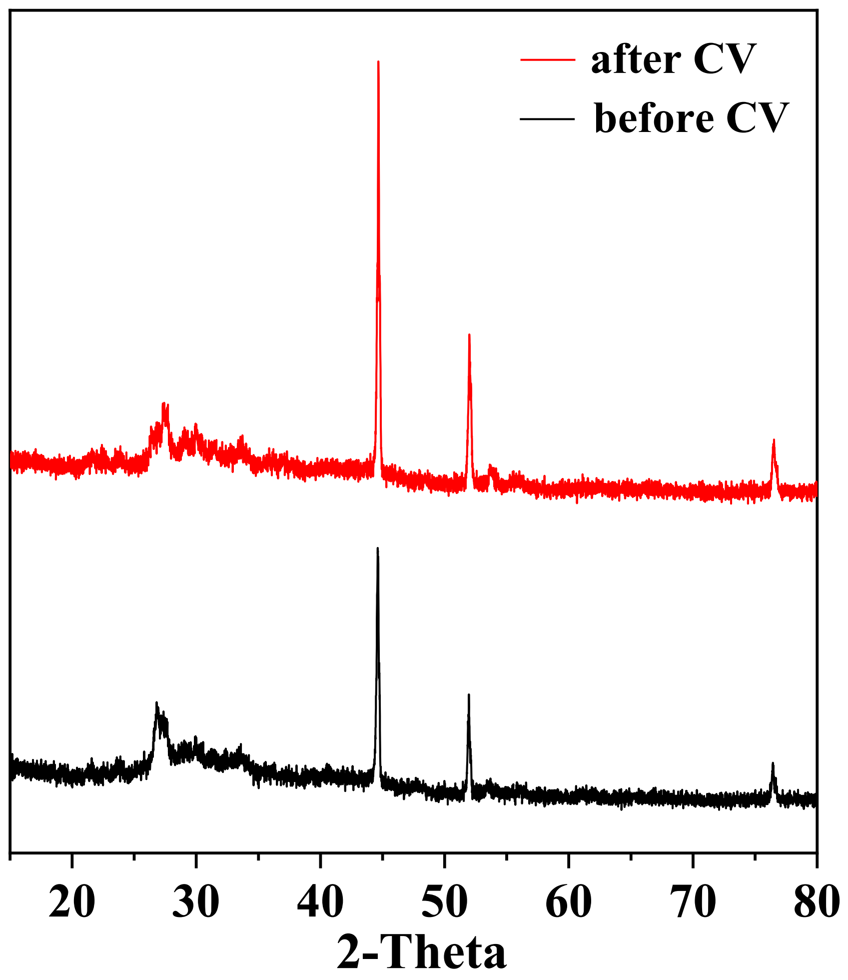

Figure S11. XRD patterns of $Ni(PO_3)_2$-MoO_3/NF before and after stability test.

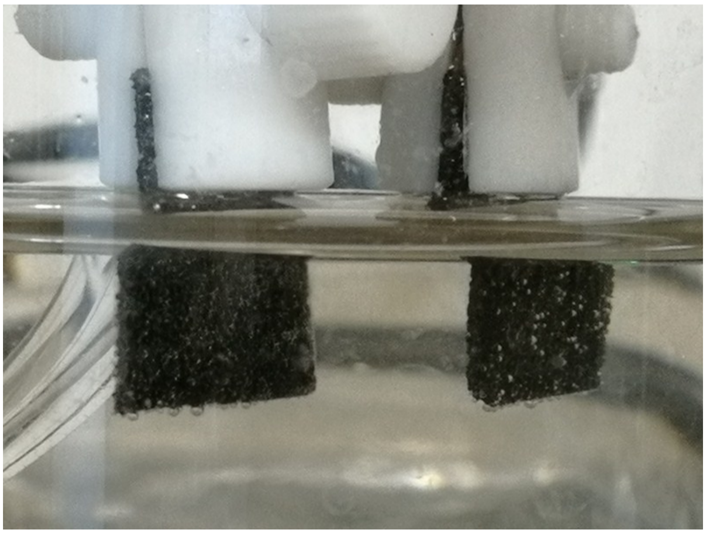

Figure S12. The photograph of bubbles during the water splitting tests.

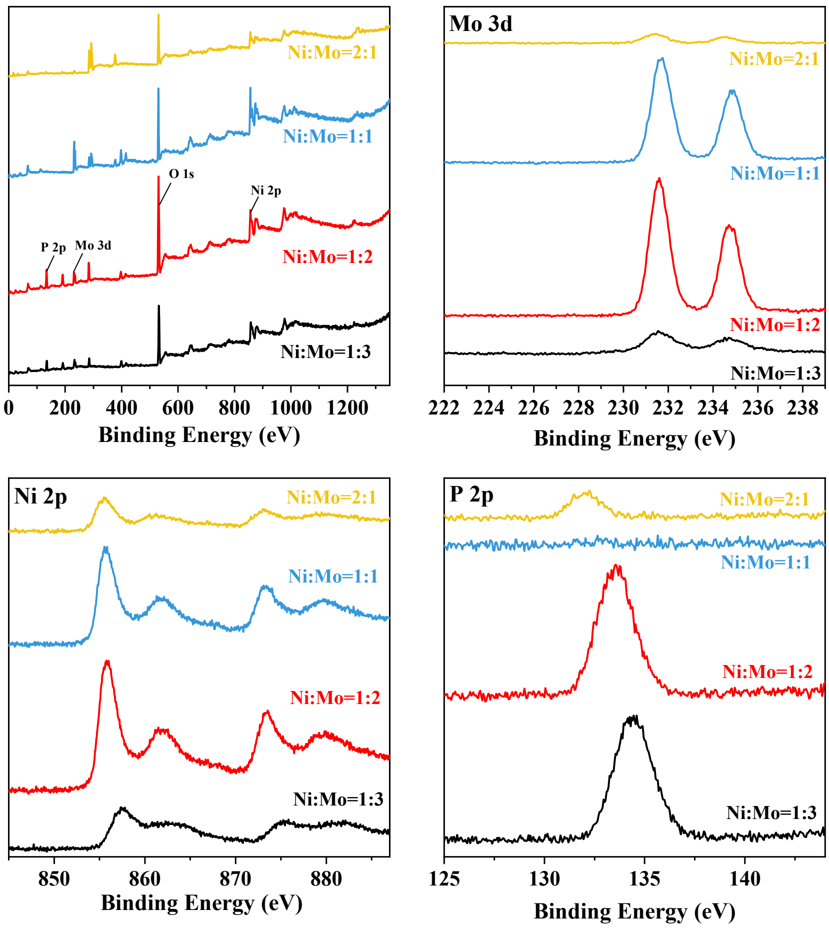

Figure S13. XPS spectrum of $Ni(PO_3)_2$-MoO_3/NF from different ratio of Ni:Mo.

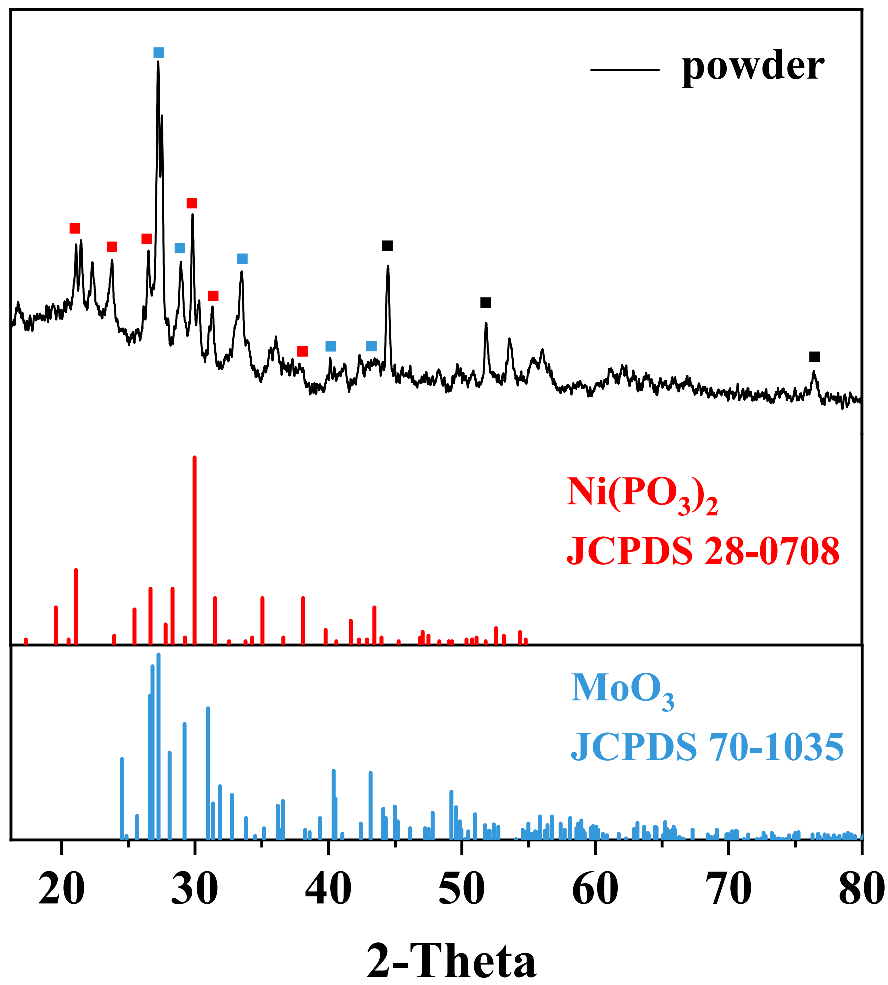

Figure S14. XRD patterns of $Ni(PO_3)_2$-MoO_3 powder.

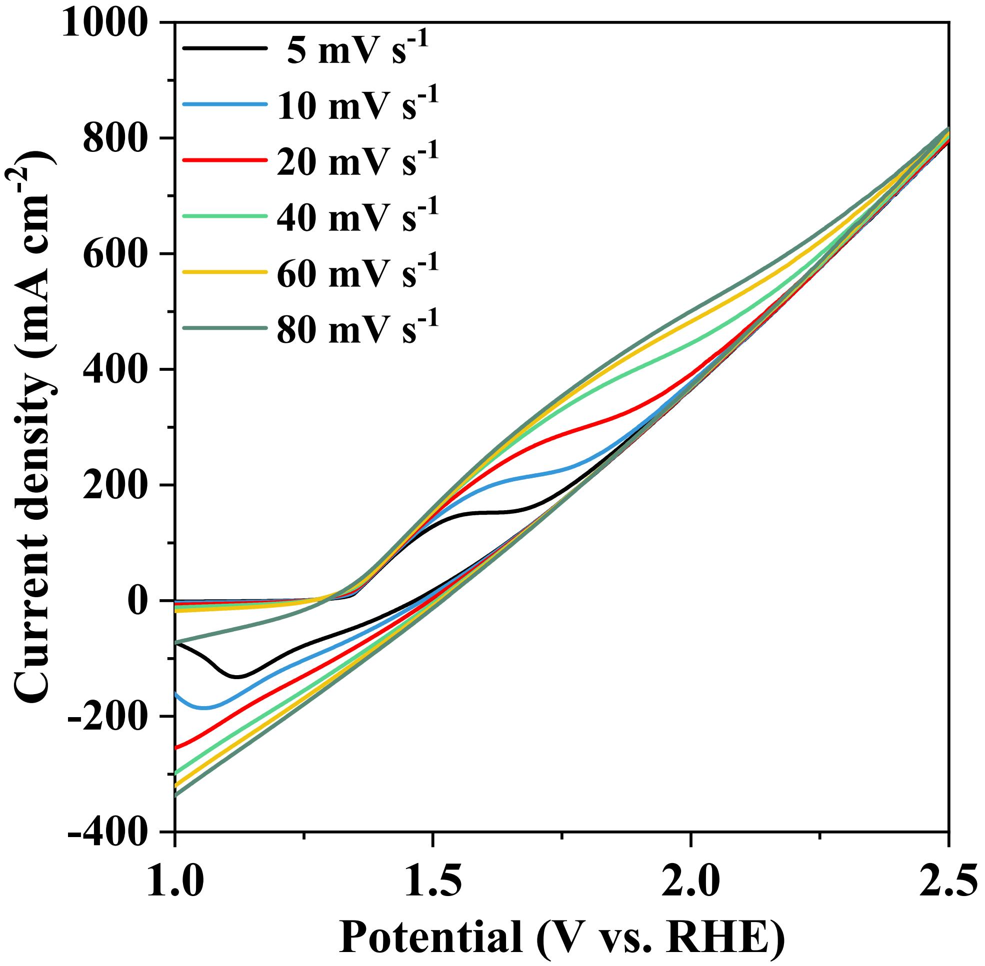

Figure S15. OER performance of $Ni(PO_3)_2$-MoO_3/NF in different scan rates.

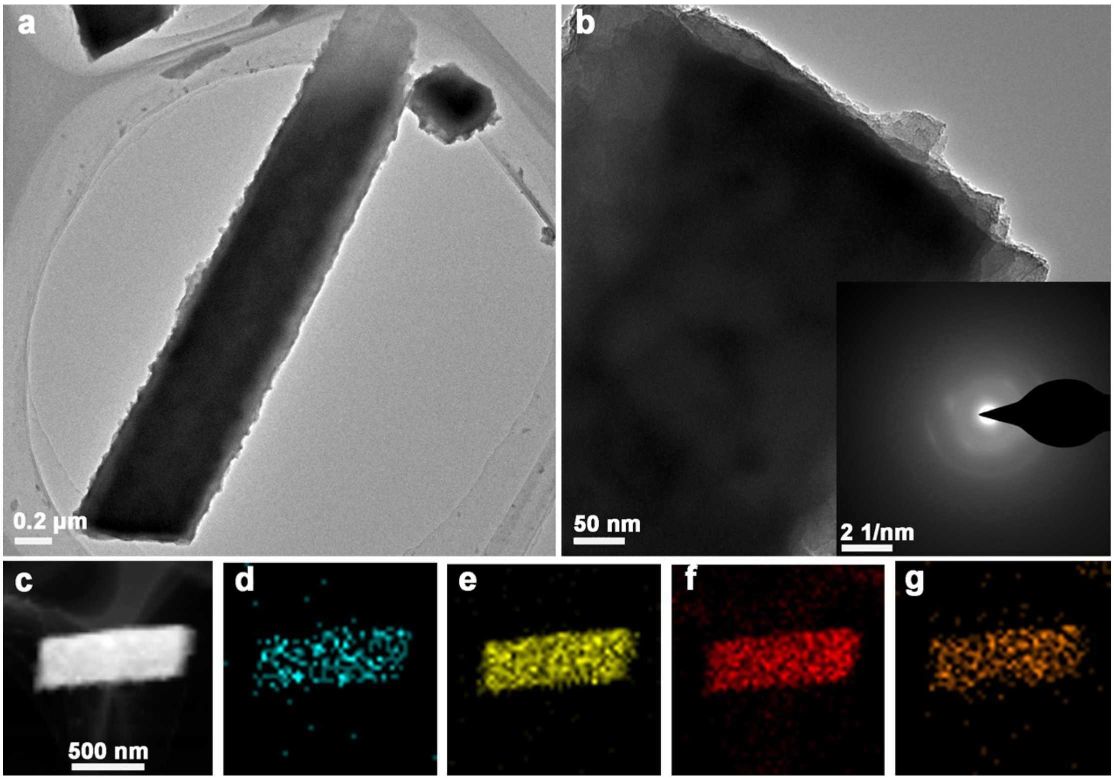

Figure S16. (a) TEM image, (b) HRTEM image and (c-g) STEM mapping images of $Ni(PO_3)_2$-MoO_3/NF after OER. The inset in (b) shows the corresponding SAED patterns.

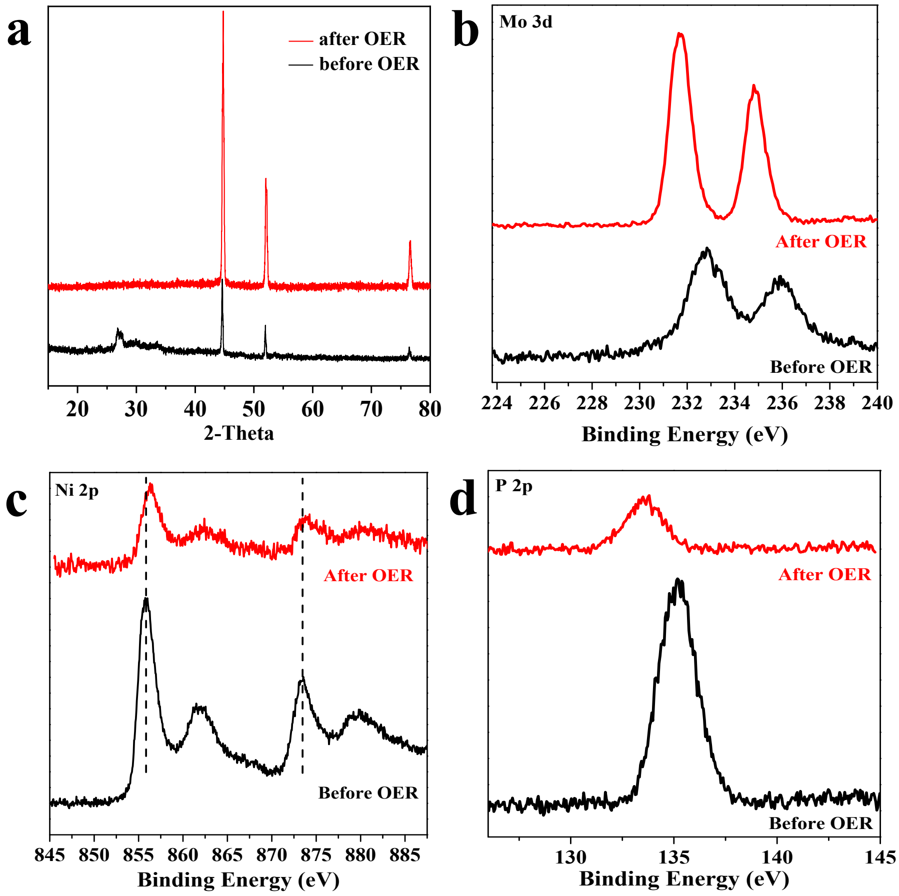

Figure S17. (a) XRD patterns and (b-d) XPS spectrum of $Ni(PO_3)_2$-MoO_3/NF after OER.

Table S1. Comparison of water splitting performance for $Ni(PO_3)_2$-MoO_3/NF with other reported electrocatalysts.

Catalyst	Current density [mA cm^{-2}]	Potential [V vs. RHE]	Electrolyte	Ref.
$Ni(PO_3)_2$-MoO_3/NF	10	1.47	1.0 M KOH	This work
$NiP_{0.62}S_{0.38}$	10	1.52	1.0 M KOH	*J. Mater. Chem. A* [1]
Co_1Mn_1CH/NF	10	1.68	1.0 M KOH	*J. Am. Chem. Soc* [2]

$Ni_2P/MoO_2@MoS_2$	10	1.56	1.0 M KOH	*Nanoscale* [3]
MoS_2/Ni_3S_2	10	1.56	1.0 M KOH	*Angew. Chem., Int. Ed. Engl.*[4]
$N\text{-}Ni_3S_2/NF$	10	1.48	1.0 M KOH	*Adv. Mater.*[5]
$MoP/Ni_2P/NF$	10	1.55	1.0 M KOH	*J. Mater. Chem. A* [6]
NiFeMo	10	1.45	1.0 M KOH	*ACS Energy Lett.*[7]
NiCoP/NF	10	1.58	1.0 M KOH	*Nano Lett.*[8]
$Co_9S_8@MoS_2/CNFs$	10	1.67	1.0 M KOH	*ACS Appl. Mater. Interfaces* [9]
$Nifoam@Ni{-}Ni_{0.2}Mo_{0.8}N$	10	1.49	1.0 M KOH	*ACS Appl. Mater. Interfaces* [10]
NiFe-NCs	10	1.67	1.0 M KOH	*ACS Appl. Mater. Interfaces* [11]
$Ni_3FeN/r\text{-}GO$	10	1.60	1.0 M KOH	*ACS Nano* [12]
CoP/rGO	10	1.70	1.0 M KOH	*Chem. Sci.*[13]
$Ni_{11}(HPO_3)_8(OH)_6$	10	1.60	1.0 M KOH	*Energy Environ. Sci.*[14]
Ni_2P	10	1.63	1.0 M KOH	*Energy Environ. Sci.*[15]
NiFeV	10	1.59	1.0 M KOH	*Small* [16]
FeS_2/CoS_2	10	1.47	1.0 M KOH	*Small* [17]
Ni@NiO	10	1.71	1.0 M KOH	*Small* [18]

Reference

1 J. Luo, H. Wang, G. Su, Y. Tang, H. Liu, F. Tian and D. Li, *Journal of Materials Chemistry A*, 2017, **5**, 14865-14872.

2 T. Tang, W. J. Jiang, S. Niu, N. Liu, H. Luo, Y. Y. Chen, S. F. Jin, F. Gao, L. J. Wan and J. S. Hu, *J Am Chem Soc*, 2017, **139**, 8320-8328.

3 Y. Wang, T. Williams, T. Gengenbach, B. Kong, D. Zhao, H. Wang and C. Selomulya, *Nanoscale*, 2017, **9**, 17349-17356.

4 J. Zhang, T. Wang, D. Pohl, B. Rellinghaus, R. Dong, S. Liu, X. Zhuang and X. Feng, *Angew*

Chem Int Ed Engl, 2016, **55**, 6702-6707.
5 P. Chen, T. Zhou, M. Zhang, Y. Tong, C. Zhong, N. Zhang, L. Zhang, C. Wu and Y. Xie, *Adv Mater*, 2017, **29**.
6 C. Du, M. Shang, J. Mao and W. Song, *Journal of Materials Chemistry A*, 2017, **5**, 15940-15949.
7 F. Qin, Z. Zhao, M. K. Alam, Y. Ni, F. Robles-Hernandez, L. Yu, S. Chen, Z. Ren, Z. Wang and J. Bao, *ACS Energy Letters*, 2018, **3**, 546-554.
8 H. Liang, A. N. Gandi, D. H. Anjum, X. Wang, U. Schwingenschlogl and H. N. Alshareef, *Nano Lett*, 2016, **16**, 7718-7725.
9 J. Bai, T. Meng, D. Guo, S. Wang, B. Mao and M. Cao, *ACS Appl Mater Interfaces*, 2018, **10**, 1678-1689.
10 J. Jia, M. Zhai, J. Lv, B. Zhao, H. Du and J. Zhu, *ACS Appl Mater Interfaces*, 2018, DOI: 10.1021/acsami.8b09854.
11 A. Kumar and S. Bhattacharyya, *ACS Appl Mater Interfaces*, 2017, **9**, 41906-41915.
12 Y. Gu, S. Chen, J. Ren, Y. A. Jia, C. Chen, S. Komarneni, D. Yang and X. Yao, *ACS Nano*, 2018, **12**, 245-253.
13 L. Jiao, Y.-X. Zhou and H.-L. Jiang, *Chem. Sci.*, 2016, **7**, 1690-1695.
14 P. W. Menezes, C. Panda, S. Loos, F. Bunschei-Bruns, C. Walter, M. Schwarze, X. Deng, H. Dau and M. Driess, *Energy & Environmental Science*, 2018, **11**, 1287-1298.
15 L.-A. Stern, L. Feng, F. Song and X. Hu, *Energy & Environmental Science*, 2015, **8**, 2347-2351.
16 K. N. Dinh, P. Zheng, Z. Dai, Y. Zhang, R. Dangol, Y. Zheng, B. Li, Y. Zong and Q. Yan, *Small*, 2018, **14**.
17 Y. Li, J. Yin, L. An, M. Lu, K. Sun, Y. Q. Zhao, D. Gao, F. Cheng and P. Xi, *Small*, 2018, **14**, e1801070.
18 H. Sun, Z. Ma, Y. Qiu, H. Liu and G. G. Gao, *Small*, 2018, DOI: 10.1002/smll.201800294, e1800294.